Hydrol. Earth Syst. Sci., 13, 577–593, 2009
www.hydrol-earth-syst-sci.net/13/577/2009/

Hydrology and Earth System Sciences

On the role of the runoff coefficient in the mapping of rainfall to flood return periods

A. Viglione, R. Merz, and G. Blöschl

Institut für Wasserbau und Ingenieurhydrologie, Technische Universität Wien, Wien, Austria

Received: 22 December 2008 – Published in Hydrol. Earth Syst. Sci. Discuss.: 30 January 2009
Revised: 28 April 2009 – Accepted: 4 May 2009 – Published: 12 May 2009

Abstract. While the correspondence of rainfall return period T_P and flood return period T_Q is at the heart of the design storm procedure, their relationship is still poorly understood. The purpose of this paper is to shed light on the controls on this relationship examining in particular the effect of the variability of event runoff coefficients. A simplified world with block rainfall and linear catchment response is assumed and a derived flood frequency approach, both in analytical and Monte-Carlo modes, is used. The results indicate that T_Q can be much higher than T_P of the associated storm. The ratio T_Q/T_P depends on the average wetness of the system. In a dry system, T_Q can be of the order of hundreds of times of T_P. In contrast, in a wet system, the maximum flood return period is never more than a few times that of the corresponding storm. This is because a wet system cannot be much worse than it normally is. The presence of a threshold effect in runoff generation related to storm volume reduces the maximum ratio of T_Q/T_P since it decreases the randomness of the runoff coefficients and increases the probability to be in a wet situation. We also examine the relation between the return periods of the input and the output of the design storm procedure when using a pre-selected runoff coefficient and the question which runoff coefficients produce a flood return period equal to the rainfall return period. For the systems analysed here, this runoff coefficient is always larger than the median of the runoff coefficients that cause the maximum annual floods. It depends on the average wetness of the system and on the return period considered, and its variability is particularly high when a threshold effect in runoff generation is present.

Correspondence to: A. Viglione
(viglione@hydro.tuwien.ac.at)

1 Introduction

In catchments with limited streamflow data or subject to major land use changes, the estimation of the design flood, i.e., the largest flood that should be considered in the evaluation of a given project, is typically performed using the *design storm procedure*. In this procedure, a particular storm with a known return period is used as an input to a rainfall-runoff model (e.g. Pilgrim and Cordery, 1993, p. 9.13), and it is then assumed that the simulated peak discharge has the same return period as the storm (e.g. Packman and Kidd, 1980; Bradley and Potter, 1992). This is a pragmatic assumption but clearly not always correct because it does not account for the role of different processes in determining the relationship between the frequencies of the design rainfall and the derived flood peak (Pilgrim and Cordery, 1975, p. 81). This relationship, hereafter referred to as *mapping of rainfall to flood return periods*, is the result of the interplay of many controls which include storm rainfall intensity, storm duration, temporal and spatial rainfall patterns, and antecedent soil moisture conditions.

Due to the complexity of the problem, we examine here a simplified world in which the effects of the processes on the mapping of return periods are more transparent than in the real world. In Viglione and Blöschl (2009) we have considered the basic case where only the storm durations play a relevant role. It was shown that, even in this very simple situation, the mapping of return periods is not trivial: except for very particular cases, the return period of the flood peak is always smaller than the return period of the generating rainfall. This is in contrast with the observations in the real world where, often, very extreme floods are produced by storms whose magnitude is not so extreme (Gutknecht et al., 2002; Reed, 1999, vol. 1, p. 32–33). The reason for this has then to be searched among other factors than the variability of storm durations. In this paper we focus on the role of the antecedent conditions of the basin expressed by the variability of the runoff coefficients.

Published by Copernicus Publications on behalf of the European Geosciences Union.

The *event runoff coefficient* is defined as the portion of rainfall that becomes direct runoff during an event. In hydrological modelling, it represents the lumped effect of a number of processes on the catchment soil moisture state (including antecedent evaporation, rainfall and snowmelt) and hence runoff. The concept of event runoff coefficients dates back to the beginning of the 20th century (e.g. Sherman, 1932) but it is still widely used for design in the engineering practice. The importance of this coefficient as a lumped indicator of the runoff generation is also confirmed by the interest of the scientific community in recent research (e.g. Naef, 1993; Gottschalk and Weingartner, 1998; Dos Reis Castro et al., 1999; Cerdan et al., 2004; Merz et al., 2006; Merz and Blöschl, 2009).

Many studies on the design storm method (e.g. Sieker and Verworn, 1980; Packman and Kidd, 1980; Pilgrim and Cordery, 1993; Alfieri et al., 2008) have concentrated on the choice of the design event, trying to fit its parameters in a way that the correspondence of storm and flood return periods is achieved in the real world. Concerning the runoff coefficient, the choice is usually made considering "average antecedent conditions" for the catchment (Pilgrim and Cordery, 1975, 1993). The use of the median value, for example, is motivated by the fact that the probability of occurrence of higher and lower values of the runoff coefficient would be equal. As stated in Pilgrim and Cordery (1993, p. 9.13) the "use of these median values in design should minimize the problem of joint probabilities and produce a flood estimate of similar probability to that of the design rainfall".

Rather than focusing on the design event, in this paper we are interested in the relationship between the return periods of the "occurring storms" and the corresponding flood peaks (which was also the topic of Viglione and Blöschl, 2009). Our focus is on the hydro-meteorological system, and all the events that may occur are considered as potential design events. In our analysis, different artificial worlds are modelled assuming simple hypotheses for the controlling processes (block rainfall and linear catchment response) from which the relationship between rainfall and flood return periods is derived. Concerning the runoff coefficients, two main situations are considered: (1) the event runoff coefficients vary independently of the storm characteristics, meaning that they are completely determined by the antecedent conditions; (2) the event runoff coefficients are related to the volume of the *flood producing storm*, i.e., the storm that causes the flood. In both cases we analyse the relationship between the runoff coefficient and the mapping of return periods using both Monte-Carlo simulations and analytical derivations in the domain of frequency distributions. For the simplified worlds analysed here, we also derive the relation between the return periods of the input and the output of the design storm procedure when using a pre-selected runoff coefficient and the event runoff coefficient for which the one-to-one mapping is achieved and that should be used in the design storm procedure.

We first summarise the design storm procedure and define the storm return period. We then present the methods used and provide one example system of the mapping of return periods to illustrate the methods. In the results section we compare different systems with different distributions of the runoff coefficient.

2 Design-storm procedure and definition of storm return period

The idea of the design storm procedure is to estimate a flood of a selected return period from rainfall *intensity-duration-frequency* (IDF) curves for the site of interest. In many cases, the hydrological engineer has standard IDF curves available for the site but it is important to understand the procedure used to develop them. For each duration selected, the annual maximum rainfall intensity is extracted from historical rainfall records. Then frequency analysis is applied to the annual data obtaining a return period for each intensity and duration. What is termed "duration" in the procedure is in fact not a storm duration but an aggregation time interval, or *aggregation level*. For example, if hourly rainfall data are available and one is interested in the IDF curve for an aggregation level t_{IDF}=3 h, one runs a moving averaging window of width t_{IDF} over the hourly data and extracts the largest 3-h average of each year to do the frequency analysis. The moving averaging procedure is equivalent to convoluting the rainfall time series with a rectangular filter (with a base of 3 h in the example). Using the wording of Koutsoyiannis et al. (1998), the problem of the construction of the IDF curves is not a problem of statistical analysis of a single random variable, as it includes two variables, intensity and aggregation level. Nor is it a problem of two random variables, because t_{IDF} is not a random variable. It consists of the study of a family of random variables, the maximum-annual average intensities of rainfall over different time intervals t_{IDF}.

The way the design storm method is applied varies considerably between countries (see e.g. DVWK, 1999; Pilgrim, 1987; Houghton-Carr, 1999) but the main components of the procedure can be summarised as following:

1. Selection of many storms of different durations reading off their mean intensities from the IDF curve corresponding to the return period T_P of interest. As noted above, rainfalls from the IDF curves do not represent complete storms but are from intense bursts within these storms. The storm duration t_r may hence differ from the aggregation level t_{IDF} used to read off the intensity from the IDF curve. However, in many cases storm duration is chosen equal to the aggregation level (see Chow et al., 1988, for details).

2. Application of rainfall time patterns to these storms (design hyetograph). Rigorously, the design temporal patterns need to be appropriate for the intense bursts

within storms, and not for complete storms (Pilgrim and Cordery, 1993, p. 9.13) but, again, in practice these two are often set equal.

3. Application of spatial patterns to rainfall or, more simply, of an areal reduction factor for catchment area.

4. Transformation of the design storm to a flood hydrograph using an event based runoff model calibrated for the catchment of interest and with chosen initial soil moisture conditions (which, in simple models, are represented by the event runoff coefficient).

5. Selection of the maximum flood peak of the flood hydrographs produced by storms of different durations.

It is then assumed that this flood peak has a return period T_Q equal to T_P.

When analysing occurring storms, the *storm return period* is defined as the return period which would be assigned to the storm event if it were used as input to the design storm procedure. It is indeed the maximum return period that can be assigned to a rainfall event when considering different aggregation levels, i.e., the return period read off the IDF curve for the aggregation level corresponding to the main burst of the storm, and hence equal to T_P.

In the real world applications of the design storm procedure, there is no rigorous solution to the problem of choosing the design parameters (i.e., the shape of the hyetograph, the rainfall-runoff model parameters, etc.) in a way that T_Q matches T_P because of the large number of controls that are difficult to understand. In contrast, when a simplified world is assumed, the exact mapping of rainfall to flood return periods can be derived. In the case of block rainfall, as assumed here, the total rainfall event and the main burst are indeed identical, so the aggregation level used to evaluate the return period of a storm is equal to the duration of that storm ($t_{\mathrm{IDF}}=t_r$).

3 Method and one example system

We use here a simplified version of the rainfall and rainfall-runoff models presented in Sivapalan et al. (2005). Essentially, the rainfall model consists of uniform and independent events whose durations t_r and intensities i are random and mutually dependent. Other factors such as multiple storms, within-storm intensity patterns, seasonality and spatial variability of the rainfall intensities are deliberately neglected for clarity. The lumped rainfall-runoff model considers the runoff routing component as a linear reservoir with response time t_c, with variable event runoff coefficients and without accounting for a base flow component. The runoff coefficient is always assumed constant during the event but is allowed to vary between events. In Appendix A more details on the rainfall and rainfall-runoff models are provided.

To be consistent with the design storm method, the return period T_P of a block storm of duration t_r is defined as the inverse of the exceedance probability of its intensity i on the distribution of maximum annual rainfall intensities averaged over the aggregation level $t_{\mathrm{IDF}}=t_r$ (see Viglione and Blöschl, 2009). T_Q is the inverse of the exceedance probabi-lity of one flood peak on the distribution of maximum annual flood peaks obtained by the model. The mapping of rainfall to flood return periods is described by graphs that relate the storm return period T_P to the return period T_Q of the corresponding flood peak (i.e., the same event).

We use two approaches to derive flood frequencies from rainfall: Monte-Carlo simulations and an analytical approach. In Fig. 1 a comparison between the two approaches is provided for one particular system. To produce Panels (a) and (b), the following Monte-Carlo approach has been used:

1. Synthetically generate N years (e.g. N=100 000) of rainfall events using the rainfall model of Appendix A (Eqs. A1 and A4);

2. Calculate the IDF curves from all storms;

3. For each event, draw a runoff coefficient r_c from a beta distribution (see Sect. 4) and apply it to calculate runoff (Eq. A8 in Appendix A);

4. Scan the resulting events and pick the largest flood peak and the flood producing storm (i.e., the storm responsible for this flood) for each year;

5. Calculate the return period of all the flood peaks by the Weibull plotting position formula;

6. Evaluate the return period T_P of the flood producing storms comparing their intensities with the IDF values corresponding to their durations (for $t_{\mathrm{IDF}}=t_r$).

The points in Fig. 1a show the 100 000 maximum annual floods. The colours represent the event runoff coefficients: dark blue corresponds to large runoff coefficients, light yellow to low runoff coefficients. As would be expected, the dark blue points concentrate in the upper part of the graph, meaning that high runoff coefficients are responsible for high flood return periods. However, a number of large runoff coefficients are associated with low T_Q because the durations of these storms are very different from the *critical storm duration* t_r^* (see Viglione and Blöschl, 2009).

Panel (b) has been obtained by slicing Fig. 1a by horizontal planes, and plotting the ratio between the return periods T_Q/T_P vs. the storm duration normalised by the basin response time (t_r/t_c). For the slices, flood return periods between 50 and 200 years have been selected to represent the $T_Q \approx 100$ years case. As explained in Viglione and Blöschl (2009), the maximum of the return period ratios is due to the interplay between catchment processes and rainfall processes and occurs at a critical storm duration t_r^*. The maximum occurs for the highest runoff coefficients.

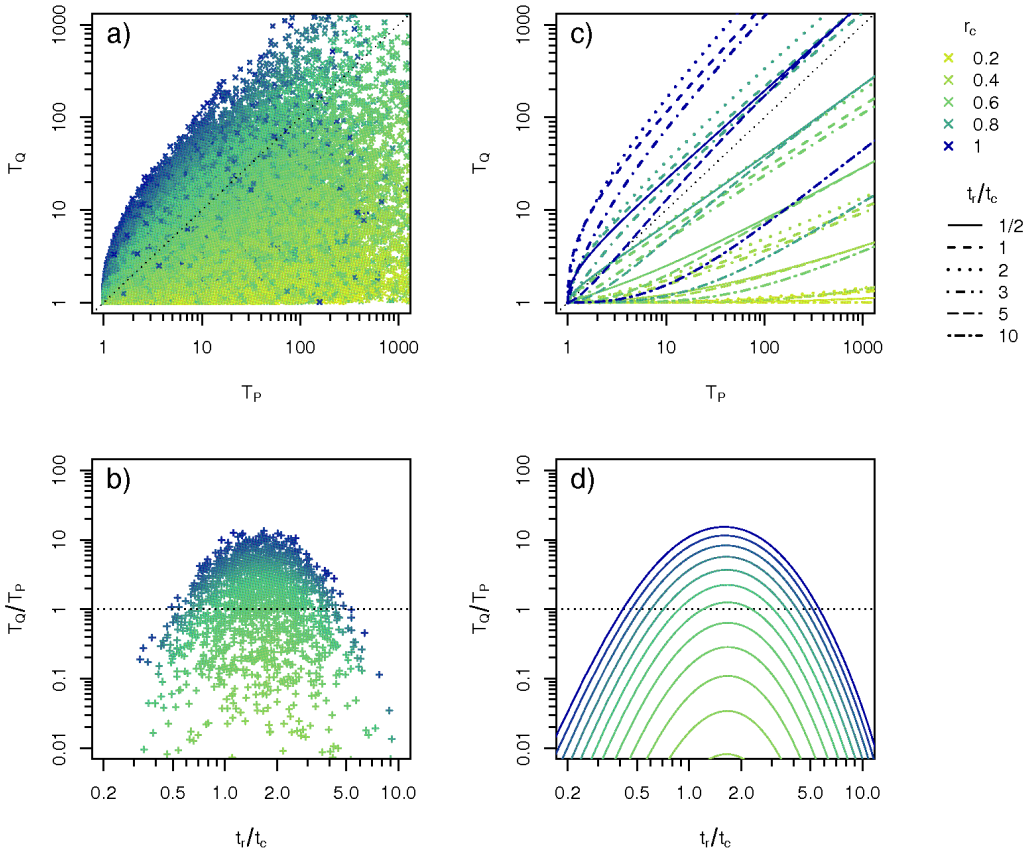

Fig. 1. Relationship between rainfall return periods T_P and flood return periods T_Q: Monte-Carlo simulation vs. analytical derivation. Panel (a) shows the mapping of return periods obtained simulating 100 000 years of events. Events characterized by high runoff coefficients r_c are dark-blue while low r_c events are represented in light-green. In Panel (c) the same system is analysed by the derivation in the domain of frequency distributions. Each line corresponds to events with the same runoff coefficient (colour) and the same storm duration (line-type). Horizontal slices for T_Q=100 years are represented in terms of T_Q/T_P in Panels (b) and (d) as a function of the storm duration t_r normalised by the basin response time t_c.

Panels (c) and (d) depict the same situation, but the derivation is performed in the domain of the frequency distributions. We use the same approach explained in Viglione and Blöschl (2009), with the only difference that the runoff coefficients r_c are allowed to vary randomly (see Appendix B) while Viglione and Blöschl (2009) used a constant runoff coefficient. Random runoff coefficients make the analytical derivation of the flood frequency distribution more complex (see Appendix B1) while the IDF-based methodology is the same as presented in Viglione and Blöschl (2009) (see Appendix B2). In Fig. 1c the mapping of T_P and T_Q is evaluated for five runoff coefficients (r_c=0.2, 0.4, 0.6, 0.8, 1) and six storm durations (t_r/t_c=1/2, 1, 2, 3, 5, 10). This gives thirty lines with colours relating to r_c (as in Panel a) and line-types relating to t_r. The figure clearly shows that the mapping of the return periods is a function of both t_r and r_c. In particular, the *envelope curve*, corresponding to the most critical events, has runoff coefficients equal to 1 and a critical storm duration t_r^*. This curve is a maximum that cannot be exceeded (for any duration t_r and runoff coefficient r_c). The analytical derivation gives the relationship between T_P and T_Q of any event of given t_r and r_c in a particular system, corresponding to the application of the design storm method, but gives no information about the probability that such an event happens. An estimation of this probability can be obtained from the Monte-Carlo simulation of Panel (a), as it is related to the density of points.

Panel (d) is analogous to Panel (b) but shows the maximum more clearly to occur around a critical duration of $t_r^* \approx 1.8\, t_c$ for all the runoff coefficients. This is similar to the case of constant runoff coefficients and is explained in Viglione and Blöschl (2009).

4 Results: comparison between systems

Different hypotheses on the distribution of the runoff coefficient r_c are formulated in the following. Two main situations are considered: in Sect. 4.1 the event runoff coefficient

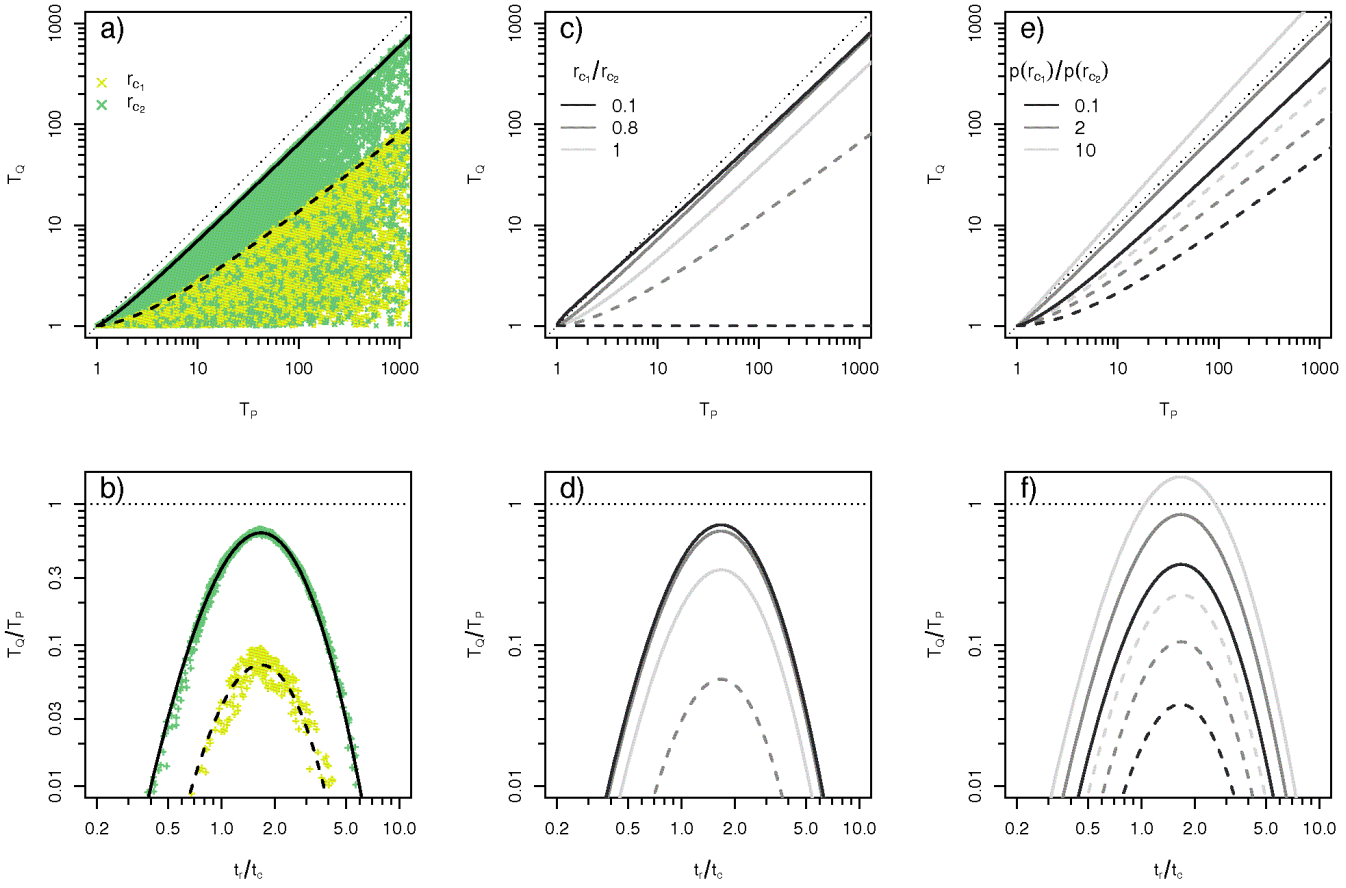

Fig. 2. Relationship between rainfall return periods T_P and flood return periods T_Q for two possible runoff coefficients $r_{c_1}<r_{c_2}$. Panel (a) – Mapping of return periods and envelope curves for r_{c_1}=0.45 (dashed line) and r_{c_2}=0.55 (continuous line) with equal probabilities $p(r_{c_1})=p(r_{c_2})$=0.5; Panel (b) – Horizontal slice of Panel (a) in terms of T_Q/T_P for T_Q=100; Panels (c) and (d) – Sensitivity to the ratio r_{c_1}/r_{c_2} (only the envelope curves are drawn) when $p(r_{c_1})=p(r_{c_2})$=0.5; Panels (e) and (f) – Sensitivity to the ratio of probabilities $p(r_{c_1})/p(r_{c_2})$ (only the envelope curves are drawn) when r_{c_1}=0.45 and r_{c_2}=0.55. In all the figures, we use colours when one system is represented and the grey scale when many systems are compared.

varies independently of the storm characteristics, while in Sect. 4.2 it is related to the volume of the flood producing storm through a threshold effect. The first case is motivated by the results of Merz and Blöschl (2009) that indicate that the runoff coefficients tend to be more controlled by antecedent soil moisture than by rainfall event characteristics. The second case is motivated by the importance of threshold effects in runoff generation reported in the literature (Western et al., 1998; Zehe and Blöschl, 2004; Struthers and Sivapalan, 2007; Zehe et al., 2007; Kusumastuti et al., 2007). In both cases, we analyse first the simple situation where only two runoff coefficients can occur, which is a small extension to the constant runoff coefficient case of Viglione and Blöschl (2009). Next we analyse the more realistic case of continuous variability of the runoff coefficients. Finally, we examine what is the result of different choices for the runoff coefficient in the design storm method and what runoff coefficients give a 1:1 correspondence of T_P and T_Q.

4.1 Event runoff coefficients independent of the event storms

4.1.1 Two possible runoff coefficients

Suppose that only two runoff coefficients r_{c_1}=0.45 and r_{c_2}=0.55 are possible with occurrence probabilities $p(r_{c_1})=p(r_{c_2})$=1/2. A Monte-Carlo simulation of such a situation is shown in Fig. 2 (Panels a and b), where the light-green points represent r_{c_1}=0.45 and the dark-green points r_{c_2}=0.55. Obviously, for a given storm intensity and duration, the events with r_{c_2} produce larger floods. The two black envelope curves in Panel (a) are derived analytically. They represent the result of the design storm procedure in such a system when using r_{c_1} (dashed line) or r_{c_2} (continuous line) as design runoff coefficient. The situation is also shown as a slice with $T_Q \approx$100 years (Panel b). Similar to the case of constant runoff coefficients (Viglione and Blöschl, 2009), the ratio between the return periods increases with

storm duration, reaches a maximum, and decreases for larger durations. The maximum is reached at $t_r/t_c \approx 1.8$ for the events with the large runoff coefficients r_{c_2}. However, T_Q/T_P is always below 1 which is a similar result as the constant runoff coefficient case of (Viglione and Blöschl, 2009).

In Panels (c) and (d) different systems are compared in order to investigate the sensitivity to the ratio r_{c_1}/r_{c_2} of the mapping of the return periods using the analytical derived distribution approach. In Panel (c) the two envelope curves are shown for each system: the curve of the events with critical storm duration t_r^* and the small runoff coefficient r_{c_1} (dashed lines), and the curve of the events with critical storm duration t_r^* and the large runoff coefficient r_{c_2} (continuous lines). The light-grey curve corresponds to $r_{c_1}=r_{c_2}$ and is the one obtained in Viglione and Blöschl (2009) (i.e., constant runoff coefficients). For $r_{c_1}=0.8\,r_{c_2}$ there is a separation into two curves, one above and one below the light-grey line of the basic system with constant runoff coefficient. By increasing the difference between r_{c_1} and r_{c_2}, the distance between the upper and the lower curves increases but the maximum T_Q/T_P does not exceed a threshold that is almost always below the 1 to 1 line. The same situation is reflected in Panel (d) considering T_Q=100 years and different storm durations.

Figure 2e and f examine instead different occurrence probabilities $p(r_{c_1})$ and $p(r_{c_2})$ when r_{c_1}=0.45 and r_{c_2}=0.55. In the "drier system", where the probability of having a low runoff coefficient is high ($p(r_{c_1})/p(r_{c_2})$=10), the ratio T_Q/T_P is greater than in the "wetter system" ($p(r_{c_1})/p(r_{c_2})$=0.1). This could appear as counter intuitive but has a simple justification: in the wetter system it is normal to have the high runoff coefficient r_{c_2} so that heavy floods are not particularly rare. In contrast, in the drier system, occurrence of a large runoff coefficient r_{c_2} is rare and corresponds to a very unusual event (and to higher T_Q). Therefore, the envelope curve is high and can even exceed the 1:1 line.

4.1.2 Continuous distribution of runoff coefficients

Assume the runoff coefficients r_c of all the events to be a random variable, modelled according to the beta distribution as in Gottschalk and Weingartner (1998):

$$f_R(r_c) = \frac{1}{B(u,\,v)} r_c^{u-1}(1-r_c)^{v-1} \quad 0 < r_c < 1\,, \tag{1}$$

where $B(u,v)$ is the incomplete beta function. Given the mean δ_c and standard deviation σ_c of the runoff coefficients, the parameters u and v of the beta distribution can be estimated as

$$u = \frac{\delta_c^2(1-\delta_c)}{\sigma_c^2} - \delta_c\,, \tag{2}$$

$$v = \frac{\delta_c(1-\delta_c)^2}{\sigma_c^2} - (1-\delta_c)\,. \tag{3}$$

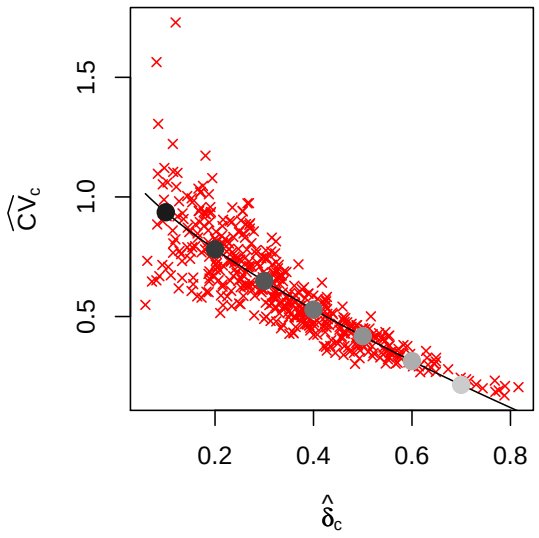

Fig. 3. Average runoff coefficient $\hat{\delta}_c$ vs. coefficient of variation $\widehat{CV}_c$ (red crosses) for 459 Austrian catchments (Fig. 1 in Merz and Blöschl, 2009). The values of δ_c and CV_c corresponding to the grey circles are used as parameters for the systems analysed in Sect. 4.1.2.

In order to consider a realistic range of distributions for the runoff coefficient, we used the database collected in Merz and Blöschl (2009) that consists of 64 461 events in 459 Austrian catchments. In Fig. 3 the sample coefficient of variation $\widehat{CV}_c$ is plotted against the sample mean event runoff coefficients $\hat{\delta}_c$ for each Austrian catchment (red crosses). There is a clear decreasing trend of CV with increasing mean runoff coefficients (continuous black line), meaning that in catchments where runoff coefficients tend to be large, the variability between the events is small. On the other hand, in catchments where runoff coefficients tend to be small, events with runoff coefficients much greater than the mean can occur, which results in a much higher CV.

Figure 4 compares three different systems characterised by different distributions of r_c: panels (a) and (b) represent a dry system having δ_c=0.1 and σ_c^2=0.009 (CV_c=0.95), Panels (c) and (d) a wetter system with δ_c=0.3 and σ_c^2=0.038 (CV_c=0.65), and Panels (e) and (f) a very wet system with δ_c=0.7 and σ_c^2=0.022 (CV_c=0.21). These three systems correspond to three of the grey points in Fig. 3 (respectively the first, the third and the last, starting from left). The simulated runoff coefficients are indicative of the type of system: the dry system has lower runoff coefficients (i.e., yellow, light-green colours), while the wet system has higher runoff coefficients (i.e., dark-green, blue colours). Looking at these graphs one question immediately arises: why does the dry system have higher T_Q/T_P? One would have expected the contrary with larger runoff coefficients and hence larger flood peaks in the wet system. The explanation is analogous to the one given for the case of two possible runoff coefficients with

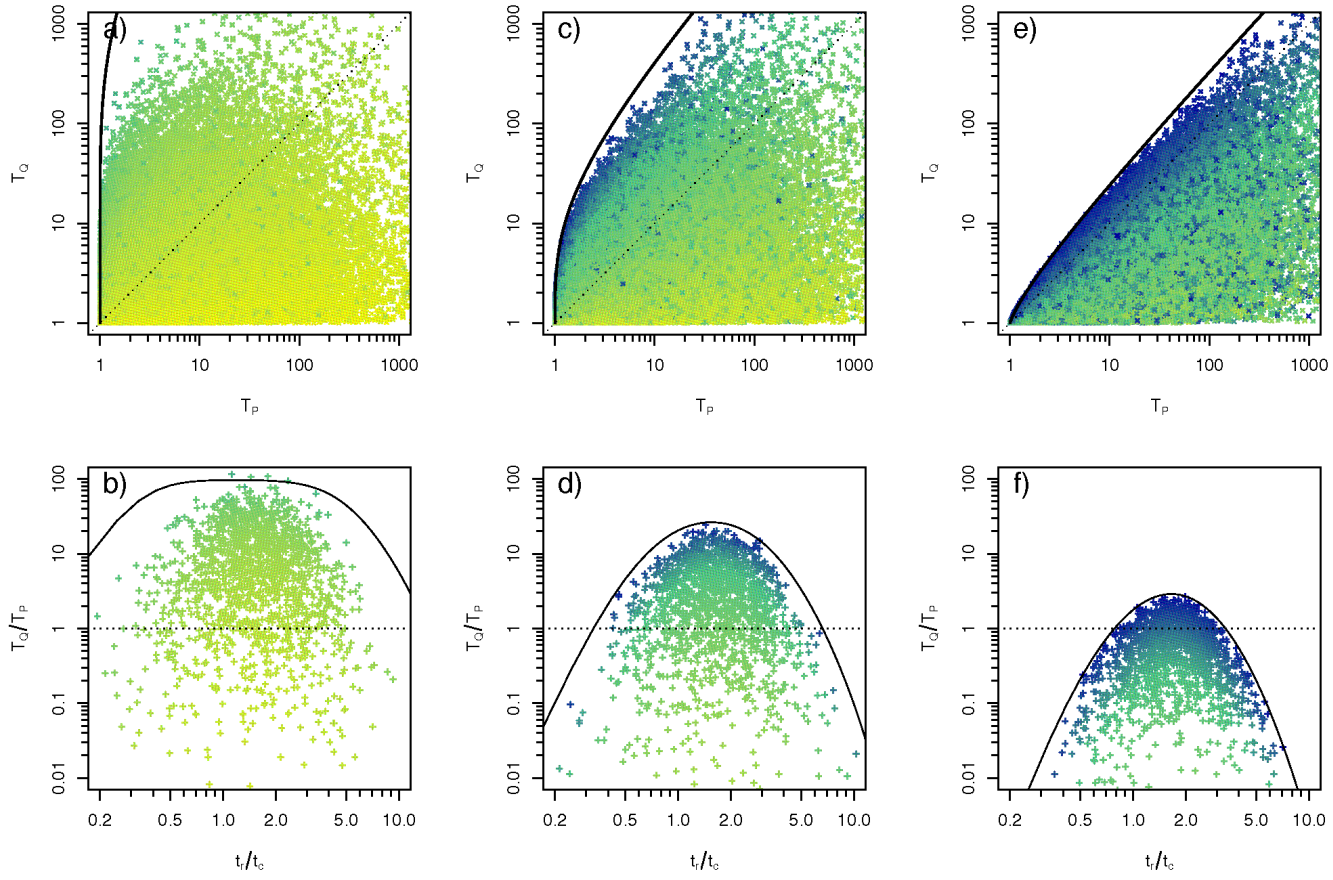

Fig. 4. Relationship between rainfall return periods T_P and flood return periods T_Q for beta distributed runoff coefficients r_c independent from the rainfall events. The three upper Panels (a), (c) and (e) represent the mapping of T_P vs. T_Q. The crosses are obtained by Monte-Carlo simulations (100 000 years). The envelope curves (continuous lines) are calculated analytically. The three lower Panels (b), (d) and (f) represent one horizontal slice (T_Q=100 years) of Panels (a), (c) and (e) respectively in terms of the ratio of return periods T_Q/T_P. The parameters of the beta distribution are: Panels (a) and (b) – Dry system with average runoff coefficient δ_c=0.1 and variance σ_c^2=0.009 (CV_c=0.95); Panels (c) and (d) – Wetter system with δ_c=0.3 and σ_c^2=0.038 (CV_c=0.65); Panels (e) and (f) – Very wet system with δ_c=0.7 and σ_c^2=0.022 (CV_c=0.21).

different probabilities. In the wet system, the flood peaks are indeed higher, because of the higher r_c, but high flood peaks are frequent (i.e., T_Q is not particularly high). In contrast, having $r_c \approx 1$ in the dry system is rare and corresponds to very unusual events (resulting in high T_Q), i.e., in dry systems the effect of the event runoff coefficient on the flood return period is larger than in wet systems. The black envelope curves of Fig. 4, for the critical storm duration t_r^* and r_c=1, are calculated by the analytical approach. The distance between these curves and the simulated events, particularly evident in the dry system of Panels (a) and (b), is related to the probability that such extreme events happen.

4.1.3 Choice of the runoff coefficient in the design storm method

In the engineering practice, when applying the design storm procedure, one is usually interested in obtaining flood peaks with the same return period as the input storms. In this section, we examine what is the result of the design storm method when choosing different runoff coefficients. In particular we comment on the result of the design storm method when choosing the commonly used median value of r_c showing that generally, in our simplified world, this does not give the correspondence $T_Q = T_P$. What runoff coefficients need to be selected in order to obtain this correspondence is calculated for different systems.

The coloured lines of Fig. 5 show the mapping corresponding to the critical storm duration t_r^* (i.e., the result of the design storm method) when different r_c are selected for the three systems (dry, wet, very wet) analysed in Fig. 4. The spacing between these lines is a measure of the sensitivity of the design storm method to the choice of the runoff coefficient. In the dry system, the result of the design storm method changes a lot for small variations of r_c, much more than in the wet case. Moreover, once the design r_c is chosen, the ratio T_Q/T_P for the dry case is not a constant but highly

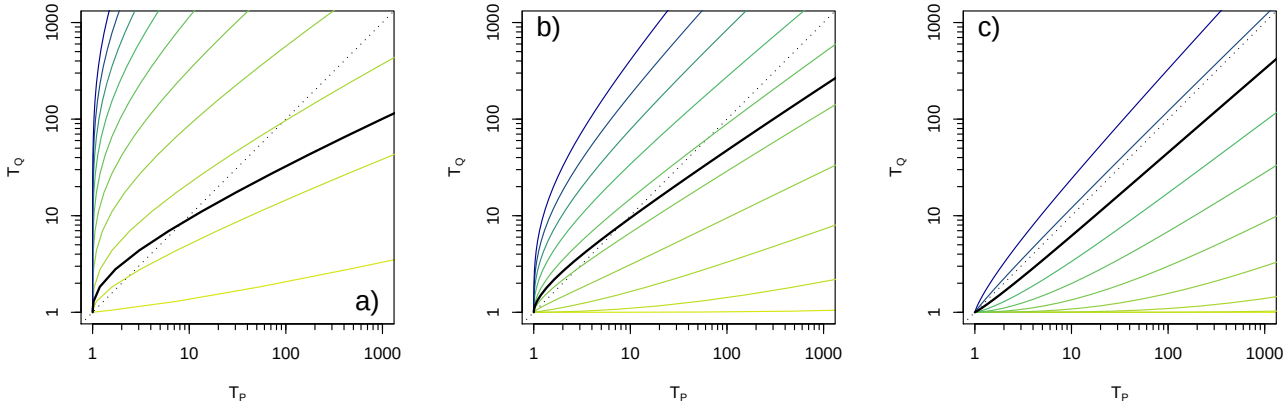

Fig. 5. Relationship between rainfall return periods T_P and flood return periods T_Q resulting from the application of the design storm method for beta distributed runoff coefficients r_c independent from the rainfall events, as in Fig. 4. The coloured lines correspond to the critical storm duration and the runoff coefficient r_c ranges from 0.1 to 1 with intervals of 0.1; the black line corresponds to the critical storm duration and the median flood producing runoff coefficient.

depends on the desired T_Q. In the wet case of Panel (c) this dependence is much weaker. This is a general result: in dry systems, great emphasis should be given to the correct choice of the design runoff coefficient when applying the design storm method, much more than in wet systems.

The black line in Fig. 5 refers to the median *flood producing runoff coefficient*, which is the median value of the runoff coefficients of the maximum annual flood events. In all three cases, using the median runoff coefficients produces flood return periods that are different from the rainfall return periods. Reading the graphs, the black line provides the storm return period T_P that should be considered to obtain a flood return period T_Q when using the median flood producing runoff coefficient in the three systems. In the dry system, one should use a value of T_P close to 1000 years to obtain T_Q=100 years and the ratio T_Q/T_P changes a lot depending on the desired T_Q (i.e., T_P should be chosen smaller than T_Q for T_Q<10 years). In the wet case, instead, one should always choose $T_P > T_Q$, e.g. $T_P \approx 300$ years to have T_Q=100 years.

Note that the median runoff coefficient highlighted as the black line in Fig. 5 is different from the median of the distribution of runoff coefficients of all flood events (Eq. 1) as only a small fraction of all events are maximum annual events. Figure 6 shows the transition from the parent distribution (all events, $f_R(r_c)$ of Panel a) to the flood producing distribution (maximum annual events, $f_R^*(r_c)$ of Panel b) of the runoff coefficients. The darkest grey shade represents the driest system, and the lightest grey shade represents the wettest system, using the same grey scale as for the points in Fig. 3.

The runoff coefficients $r_{1:1}$ (for which $T_P = T_Q$) have been back calculated from the results in Fig. 5 and are shown in Fig. 7a for the seven systems corresponding to the seven grey points in Fig. 3. Obviously, there is a big difference between

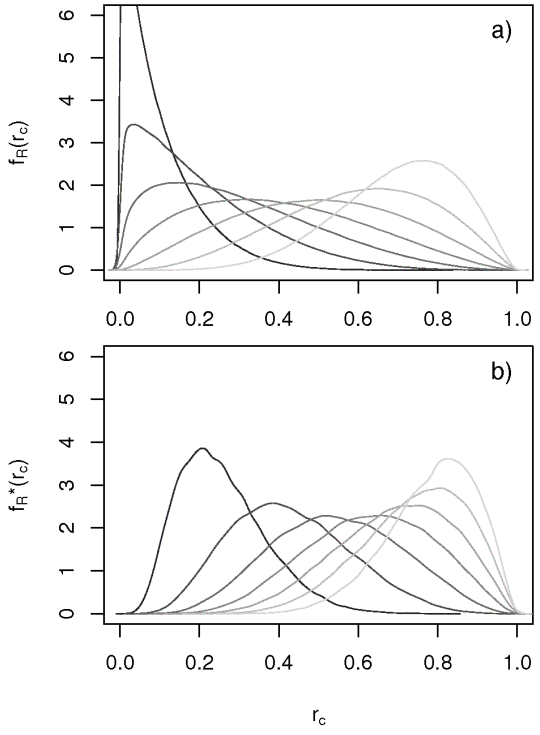

Fig. 6. Distributions of the runoff coefficients corresponding to the grey points in Fig. 3. Panel (a) – Parent distributions of the runoff coefficients $f_R(r_c)$; Panel (b) – Distributions of the flood producing runoff coefficients $f_R^*(r_c)$.

the runoff coefficients that should be used for the different cases: $r_{1:1}$ has low values for the dry systems and high values for the wet systems. Moreover, as already emerged from Fig. 5, $r_{1:1}$ varies with the return period considered: it increases with increasing magnitudes of the event, especially in the driest systems.

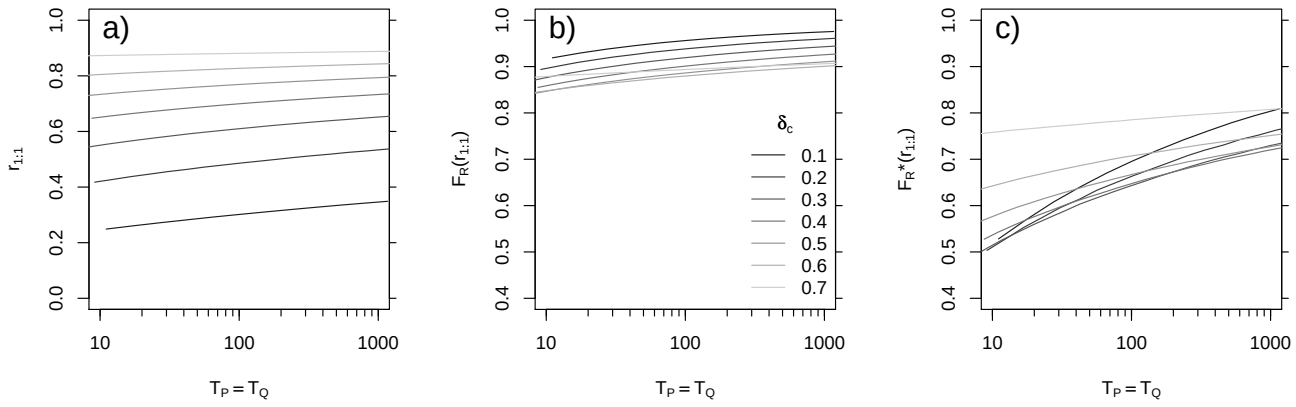

Fig. 7. Runoff coefficients $r_{1:1}$ that give a 1 to 1 correspondence between rainfall and flood return periods plotted against return period. Panel (a) – Runoff coefficient $r_{1:1}$; Panel (b) – Non-exceedance frequency of $r_{1:1}$ on the parent distributions of r_c; Panel (c) – Non-exceedance frequency of $r_{1:1}$ on the distribution of the flood producing runoff coefficients. The parent beta distributions correspond to the seven grey points in Fig. 3 (from dry to wet systems).

Panel (b) represents the probability of non-exceedance of $r_{1:1}$ corresponding to the parent distributions of r_c (i.e., all events) in Fig. 6a. For all wetness conditions and return periods, the non-exceedance probability $F_R(r_{1:1})$ of $r_{1:1}$ is around 0.9 and decreases slightly with increasing wetness of the system.

The patterns of the probability of non-exceedance of $r_{1:1}$ corresponding to the distribution of the flood producing runoff coefficients $f_R^*(r_c)$ (i.e., only the maximum annual events) is more complex. It is shown in Panel (c) and relates to Fig. 6. There is no unique non-exceedance probability of the runoff coefficients that give a 1:1 correspondence of T_P and T_Q, which depend significantly on the wetness of the system and the return period. For the driest system, $F_R^*(r_{1:1})$ significantly depends on the return period (ranging from 0.5 to 0.8), while it is almost constant and close to 0.8 for the wettest system. In all cases, however, it is evident that $r_{1:1}$ is greater than the median value of $f_R^*(r_c)$, that is represented by the black line in Fig. 5 and that would be used in a common application of the design storm method.

4.2 Non-linear relationship between flood runoff coefficients and event storm volumes: the threshold effect

Up to this point, the runoff coefficients were assumed to vary randomly, independent of storm characteristics. This section now considers a situation in which the runoff coefficient is dependent on the overall storm volume $V = i\, t_r$ through a threshold effect. Specifically, we assume that, below a fixed threshold volume V^*, the average runoff coefficient is low, while above V^* the average runoff coefficient is large. Hydrologically, this threshold effect represents, for example, the transition from saturation excess runoff to infiltration excess runoff, the activation of macropores beyond a moisture threshold, the onset of subsurface stormflow once the catchment soil moisture exceeds a threshold, or the establishment of connected flow paths within a catchment (Western et al., 1998; Zehe and Blöschl, 2004; Struthers and Sivapalan, 2007; Zehe et al., 2007; Kusumastuti et al., 2007).

4.2.1 Two possible runoff coefficients

We, again, first consider the simple case where only two runoff coefficients $r_{c_1} < r_{c_2}$ are possible. In Fig. 8, if V is under the threshold V^*, the runoff coefficient is r_{c_1}, otherwise it is r_{c_2}. This means that r_c is deterministically related to the storm volume, i.e., r_c is not fully random because its variability is determined by storm randomness. Panels (a) and (b) show the events obtained by a Monte-Carlo simulation of 100 000 years. As in Fig. 2 the light-green points represent r_{c_1}=0.45 and hence correspond to storms with volumes $V < V^*$ (with V^*=100 mm), while the dark-green points represent r_{c_2}=0.55 and volumes larger than the threshold. In Panel (b) the deterministic relationship between runoff coefficients and storm event volumes is clearly represented for a flood return period of 100 years. Short storms, that have smaller volumes, are associated with r_{c_1} and produce lower flood peaks. The transition to the long storms, responsible for the highest floods, is abrupt and is characteristic of the non-linearity of the model. The continuous lines show the results of the analytical derivation: in Panel (a) only the envelope curve is plotted; in Panel (b) the relationship (T_P, T_Q, t_r) is represented for T_Q=100 years. The shapes of the two graphs are due to the fact that the rainfall event volume depends on the rainfall intensity, which explains the subdivision between r_{c_1} and r_{c_2} in Panel (a), and on its duration, which explains the two peaks in Panel (b). In Panel (b) the transition between the two runoff coefficients is a short segment which we term *separation line*.

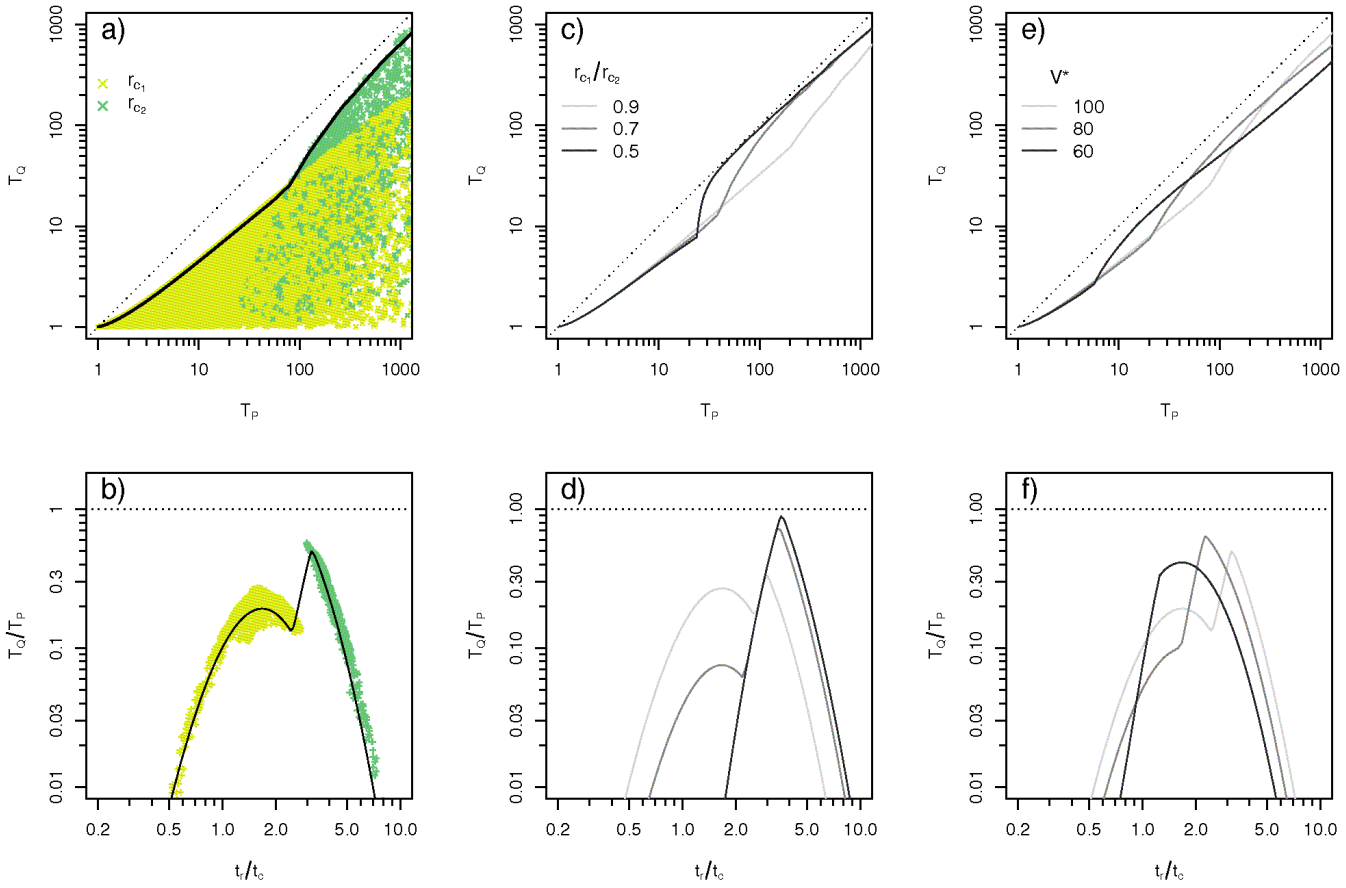

Fig. 8. Relationship between rainfall return periods T_P and flood return periods T_Q for two possible runoff coefficients r_c, where the highest one occurs when the storm volume is over the threshold V^* [mm]. The three upper Panels (a), (c) and (e) represent the mapping of T_P vs. T_Q. The crosses are obtained by Monte-Carlo simulation (100 000 years). The three lower Panels (b), (d) and (f) represent horizontal slices (T_Q=100 years) of Panels (a), (c) and (e) respectively in terms of the ratio of return periods T_Q/T_P. Panels (c) and (d) show the sensitivity to the ratio between r_{c_1} and r_{c_2}; Panels (e) and (f) show the sensitivity to the threshold V^*. In Panels (a), (b), (e) and (f) r_{c_1}=0.45 and r_{c_2}=0.55.

Panels (c) and (d) examine the sensitivity of the mapping to the ratio between r_{c_1} and r_{c_2} for a given threshold V^*=100 mm. If the ratio between the two runoff coefficients is far from unity (i.e., the runoff coefficients are dissimilar) the transition between r_{c_1} and r_{c_2} of the envelope curves shown in Panel (c) happens for small return periods. Looking at the horizontal slices of Panel (d), the difference between T_P and T_Q under and above the threshold is very different for different systems, but the separation line is always the same, as it is a consequence of the threshold only.

It is also of interest to examine the sensitivity to the threshold value. For very low and very high thresholds, the mapping of the return periods is the same (not shown here), because the systems have essentially only one possible r_c and the situation is the one examined in Viglione and Blöschl (2009). In the transition between these two extremes (Panels e and f of Fig. 8) the envelope curve is slightly higher than in the case of a single runoff coefficient, because the nonlinear threshold effect introduces some degree of variability of r_c. Panel (f) shows how the separation line depends on the threshold. For low thresholds, the line is part of the rising limb of the graph while for large thresholds it is part of the decreasing limb (viewed from left to right). The maximum ratio T_Q/T_P occurs when the separation line stays close to the critical storm duration.

4.2.2 Continuous distribution of runoff coefficients

To account for the random nature of r_c, the following assumption is made: if V is under the threshold V^*, then the runoff coefficient follows a beta distribution with mean δ_{c_1} and standard deviation σ_{c_1}; otherwise the mean is δ_{c_2} and the standard deviation σ_{c_2}. This means that the threshold volume V^* splits the (i, t_r) space into two regions where r_c has two different distributions (see Fig. B1 in Appendix B).

Some examples are given in Fig. 9 that depicts three systems where the difference between the distributions of r_c under and over the threshold is large. Below the threshold the system tends to be dry (δ_{c_1}=0.2, $\sigma^2_{c_1}$=0.024), while it tends to be wet when the threshold is exceeded (δ_{c_2}=0.6, $\sigma^2_{c_1}$=0.035).

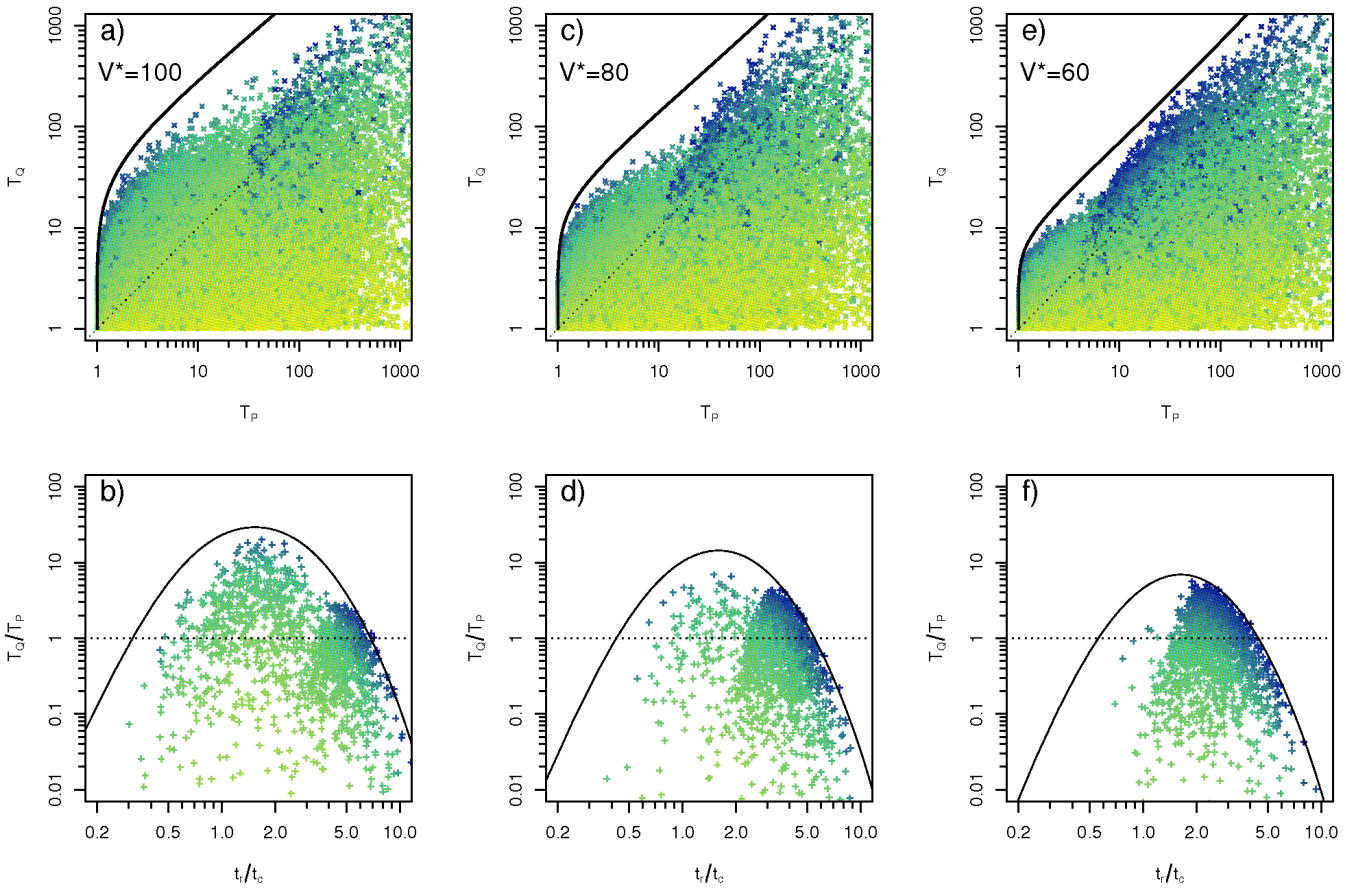

Fig. 9. Relationship between rainfall return periods T_P and flood return periods T_Q for beta distributed runoff coefficients r_c dependent on the storm volume V. Below the threshold the system tends to be dry (δ_{c_1}=0.2, $\sigma^2_{c_1}$=0.024), while it tends to be wet if the threshold is exceeded (δ_{c_2}=0.6, $\sigma^2_{c_1}$=0.035). The sensitivity to the threshold V^* [mm] is analysed. The three upper Panels (a), (c) and (e) represent the mapping of T_P vs. T_Q. The crosses are obtained by Monte-Carlo simulation (100 000 years). The three lower Panels (b), (d) and (f) represent horizontal slices (T_Q=100 years) of Panels (a), (c) and (e) respectively in terms of the ratio between return periods T_Q/T_P.

In Panels (a) and (b) the threshold V^* is high, meaning that the wet behaviour is less probable. This leads to a high envelope curve. In Panels (e) and (f), instead, the envelope curve is lower because the wet behaviour of the system is more probable (lower threshold). Panels (c) and (d) depict an intermediate situation. Similar to the case of two runoff coefficients, the abrupt switch caused by the threshold can be clearly recognised. The horizontal slices of Panels (b), (d) and (f) show that the separation line exists and corresponds to the change of density of the points. The position of the line is related to the threshold V^*.

In Panels (b) and (d) the critical storm duration t_r^* (i.e., where the maximum of T_Q/T_P occurs) corresponds to storm volumes far below the threshold V^*. This means that, for storms of duration t_r^*, the runoff coefficients belong to the distribution typical of dry systems, and events with $r_c \approx 1$ happen rarely. For t_r longer than t_r^*, V is greater than V^* and $r_c \approx 1$ can be more easily reached. If the threshold is lower, see Panel (f), t_r^* is closer to the separation line, which is the reason why the envelope curve in Panel (e) is closer to the simulated events (high r_c can be easily reached) than in Panels (a) and (c).

Figure 10 shows the effect of the threshold on the parent and the flood producing distributions of the runoff coefficients. The parent distribution $f_R(r_c)$, is hardly affected by the threshold (Panel a) causing only a small increase in the thickness of the right tail of the distribution. In contrast, the threshold significantly affects the distribution of flood producing runoff coefficients $f_R^*(r_c)$ (Panel b). This is because the flood producing storms have significant volumes to exceed the threshold regularly, while the relative number of total storms exceeding the threshold is small. For the same reason, the effect is more pronounced for small thresholds than it is for large thresholds.

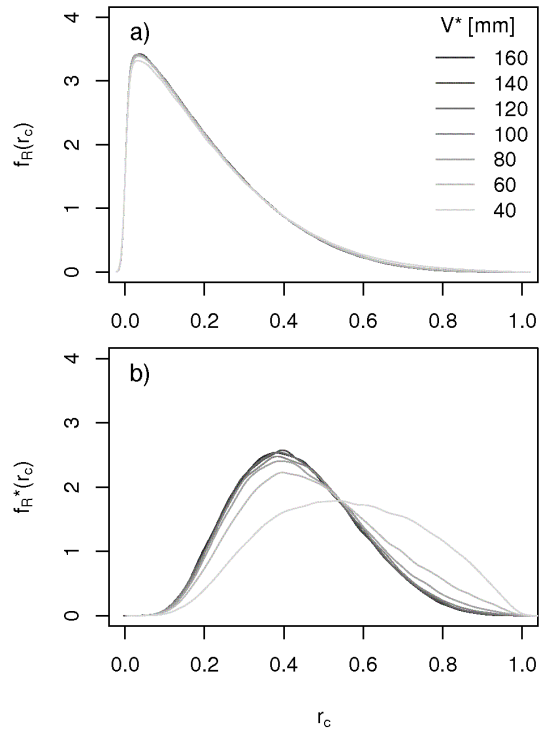

Fig. 10. Distributions of the runoff coefficients corresponding to different threshold values V^*. Below the threshold the system tends to be dry (δ_{c_1}=0.2, $\sigma^2_{c_1}$=0.024), while it tends to be wet if the threshold is exceeded (δ_{c_2}=0.6, $\sigma^2_{c_1}$=0.035). Panel (a) – Parent distributions of the runoff coefficients $f_R(r_c)$; Panel (b) – Distributions of the flood producing runoff coefficients $f^*_R(r_c)$.

4.2.3 Choice of the runoff coefficient in the design storm method

The coloured lines of Fig. 11 show the mapping corresponding to the critical storm duration t^*_r (i.e., the result of the design storm method) when different r_c are selected for the three systems analysed in Fig. 9. The black line refers to the median flood producing runoff coefficient. In all three cases, using the median runoff coefficients produces flood return periods that are very different from the rainfall return periods. Comparing Fig. 11 with Fig. 5, one sees that the ratio T_Q/T_P strongly depends on the desired T_Q when the threshold effect is present. This would be expected because of the different percentage of under-threshold and over-threshold events for different values of T_Q (see Fig. 9, Panels a, c, d), i.e., different mechanisms dominate for different flood magnitudes. The graphs can be used to select T_P so that the design storm method results in a flood with the desired return period T_Q. If considering the median flood producing runoff coefficient, with a value T_P=1000 years one would obtain $T_Q \approx$70 years in the system with high threshold, while one would obtain $T_Q \approx$20 years only in the system with low threshold volume. This is a clear example of how wrong can be the assumption $T_Q=T_P$ of the design storm method when the design runoff coefficient is not correctly selected.

In Fig. 12a the runoff coefficient $r_{1:1}$, for which $T_P=T_Q$, has been derived for different values of the threshold. The darkest line (V^*=160 mm) is very close to the line with δ_c=0.2 in Fig. 7a. Because of the high threshold V^* the system is almost always in the dry condition. The value of $r_{1:1}$ increases for decreasing thresholds from about 0.4 to about 0.8. This is because the systems change to increasingly probable wet conditions. In the limiting case of V^*=0 (not shown here) $r_{1:1}$ would correspond to the line with δ_c=0.6 in Fig. 7a (i.e., $r_{1:1}$ of about 0.8). In all the intermediate cases, because of the non-linearity of the threshold effect, $r_{1:1}$ varies a lot for varying return periods.

Panel (b) represents the probability of non-exceedance of $r_{1:1}$ in the parent distributions of r_c, i.e., the ones represented in Fig. 10a. The runoff coefficient to be used in the driest system corresponds to the lowest quantile of $f_R(r_c)$, and increases for increasing wetness of the system. This is because the parent distribution of r_c does not vary much with decreasing threshold V^*, so that higher values of $r_{1:1}$ correspond to higher quantiles (that was not the case in Fig. 7). Moreover $r_{1:1}$ is always greater than the 90% quantile ($F_R(r_{1:1})$ is between 0.9 and 1).

A similar behaviour is shown in Panel (c), representing the probability of non-exceedance of $r_{1:1}$ in the distribution of the flood producing runoff coefficients $f^*_R(r_c)$ (see Fig. 10b). Here the non-exceedance probabilities range between 0.5 and 0.9 and increase with decreasing threshold. For example, if one is to match the return periods for the case of $T_Q=T_P$=100 years, for a threshold of 160 mm one would have to choose a runoff coefficient that is exceeded in 35% of the maximum annual events, while for a threshold of 60 mm one would have to choose a runoff coefficient that is exceeded in less than 10% of the maximum annual events. If one considers the dry and wet systems of Fig. 7c corresponding to the situations below and above the threshold, the respective percentages range between around 35% and 30% depending on the average wetness of the system. In all cases $r_{1:1}$ is greater than the median value of $f^*_R(r_c)$ that is usually recommended for design flood applications.

4.3 Biases in the design storm method when assuming $T_Q=T_P$ and the median r_c

Although the focus of the paper is on return periods (i.e., on probabilities), a practical question related to our analysis of the design storm method arises: how far is the T_Q-year flood peak quantile q_{T_Q} from the flood peak $\hat{q}_{T_Q}$ obtained when applying the design storm method? We consider here the common application of the method, i.e., we assume $T_Q=T_P$ and we choose the median flood producing runoff coefficient as design value. In Table 1 the percentage bias $100(\hat{q}_{T_Q}/q_{T_Q}-1)$ has been calculated for different systems and different return periods. The three systems of Figs. 4 and

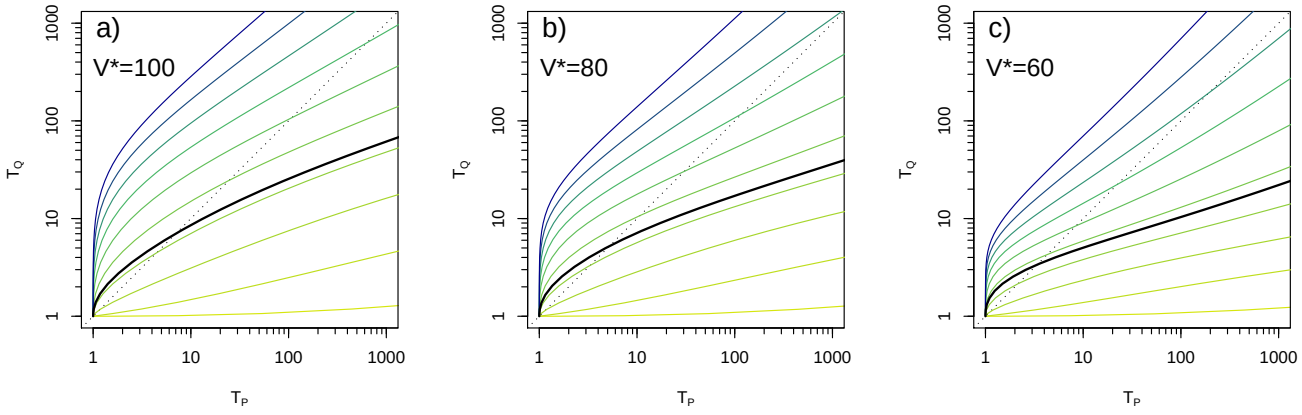

Fig. 11. Relationship between rainfall return periods T_P and flood return periods T_Q resulting from the application of the design storm method for beta distributed runoff coefficients r_c dependent on the storm volume V, as in Fig. 9. The coloured lines correspond to the critical storm duration and the runoff coefficient r_c ranges from 0.1 to 1 with intervals of 0.1; the black line corresponds to the critical storm duration and the median flood producing runoff coefficient.

5 (dry–wet) and the three systems of Figs. 9 and 11 (high–low threshold) have been considered. The percentage biases of estimation of q_{T_Q} are consistent with the mapping of the return periods represented by the black lines in Figs. 5 and 11. For the dry system, the design storm method underestimates q_{T_Q} moderately (−2.8%) when the return period of interest is 10 years but considerably more (−30%) when T_P=1000 years. On the other hand, in the wet system the bias is essentially non-affected by the desired return period and is approximately always equal to −10%. When a threshold effect in runoff generation is present, the bias of estimation of q_{T_Q} is generally greater than in the no-threshold cases. This can also be observed qualitatively comparing Figs. 5 and 11. The difference between percentage biases for low–high values of the desired return period is more pronounced when the threshold is high (i.e., when the dry situation dominates), ranging from −4.9% when T_P=10 years to −41% when T_P=1000 years. When the threshold is low (i.e., when the wet situation dominates), this difference is less evident: the percentage biases range from −26% when T_P=10 years to −44% when T_P=1000 years. This means that in a practical case of a true design value of, say, q_{T_Q}=100 m^3/s for T_Q=1000 years, the design storm method would only give $\hat{q}_{T_Q}$=60 m^3/s if runoff generation thresholds are present.

Table 1. Percentage bias of the flood peak quantile when applying the design storm method assuming T_Q=T_P and the median r_c of all maximum annual floods. The systems considered are: three systems with beta distributed runoff coefficients r_c independent of the rainfall events (Fig. 5); three systems with beta distributed runoff coefficients r_c depending on the storm volume V (Fig. 11).

	T_P=10	T_P=100	T_P=1000
Fig. 5a	−2.8%	−21%	−30%
Fig. 5b	−1.2%	−11%	−17%
Fig. 5c	−8.4%	−9.2%	−9.9%
Fig. 11a	−4.9%	−29%	−41%
Fig. 11b	−12%	−37%	−45%
Fig. 11c	−26%	−41%	−44%

5 Conclusions

In this paper we examine the effect of event runoff coefficients on the relationship between rainfall and flood return periods to shed light on design practice. We make simple hypotheses for the controlling processes (block rainfall and linear catchment response) and analyse the relationship using a derived flood frequency model in analytical and Monte-Carlo modes. Two main hydrological systems are considered: (1) the event runoff coefficient varies independently from the storm characteristics, i.e., it is determined by the antecedent conditions; (2) the event runoff coefficient is related to the volume of the flood producing storm, i.e., it is determined by the storm that causes the flood as well as antecedent conditions.

In the design storm procedure the ratio of flood and rainfall return periods T_Q/T_P is maximised by varying storm duration. Viglione and Blöschl (2009) showed that, for a system with a constant runoff coefficient, this maximum ratio is always lower than unity, being around 0.4 for $T_Q \approx$100 years. The findings in this paper indicate that allowing for variability of the runoff coefficients may increase the maximum ratio significantly. In a dry system, where high runoff coefficients are very rare, one event with a high runoff coefficient can produce a flood with a return period T_Q that is hundreds of times the return period of the corresponding storm. In a wet system, where runoff coefficients are always high, the maximum

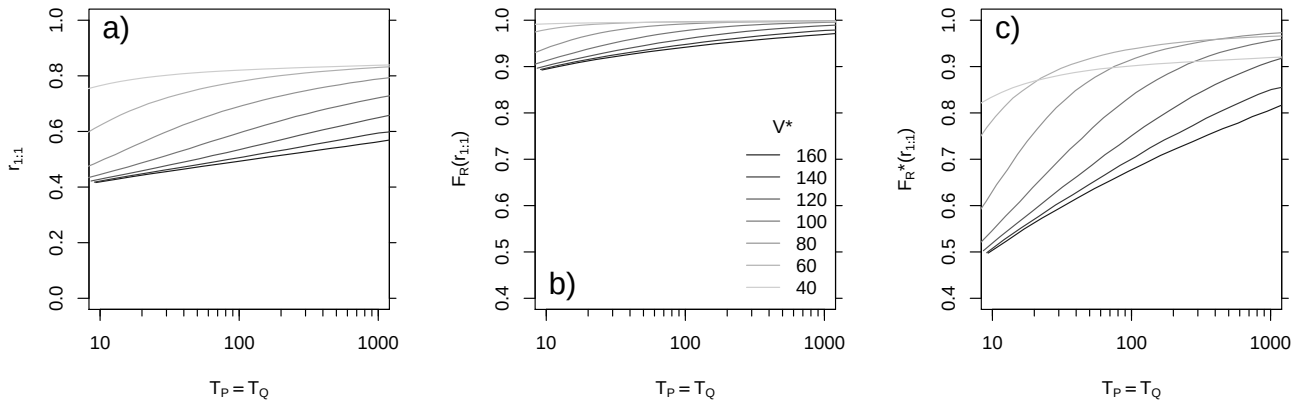

Fig. 12. Sensitivity of the runoff coefficient $r_{1:1}$ to the threshold storm volume V^* [mm]: Panel (a) – Runoff coefficient $r_{1:1}$; Panel (b) – Non-exceedance frequency of $r_{1:1}$ on the parent distributions of r_c; Panel (c) – Non-exceedance frequency of $r_{1:1}$ on the distribution of the flood producing runoff coefficients.

flood return periods are never more than a few times that of the corresponding storm. This is because a wet system cannot be much worse than it normally is.

A threshold effect in runoff generation was examined where it was assumed that, beyond a threshold rainfall volume, large runoff coefficients are more probable. Presence of a threshold effect reduces the maximum ratio of T_Q/T_P since it increases the probability of the system to be in a wet situation and decreases the randomness of the runoff coefficients in relation to the storm. If a continuous deterministic relationship between the runoff coefficient and storm volume exists (not shown here), the mapping would be the same as in the constant runoff coefficient systems examined in Viglione and Blöschl (2009). In other words, the absence of "independent randomness" of r_c in relation to the storm leads to the same mapping of return periods as a constant runoff coefficient.

Regarding the design storm method, its result when choosing a design runoff coefficient (in particular the median of the runoff coefficients that cause the maximum annual floods) has been analysed. It was shown that, in dry systems, the results of the method are much more sensitive to the chosen r_c and the desired T_Q than in wet systems. When using the median runoff coefficient, the bias of estimation of the design flood peak in the dry system ranges from -2.8% for T_Q=10 years to -30% for T_Q=1000 years. On the other hand, in the wet system the bias is essentially non-affected by the desired return period and is approximately equal to -10%. If a runoff generation threshold is present, the ratio T_Q/T_P strongly depends on the desired T_Q because different mechanisms dominate for different flood magnitudes. Also, the bias of estimation of the design flood peak is more pronounced when the threshold effect is present, reaching percentage values of -45% for a desired return period of 1000 years.

We also examined the question which runoff coefficients $r_{1:1}$ produce a flood return period equal to the rainfall return period if the design storm procedure is applied (i.e., maximising T_Q/T_P with respect to storm duration). For the systems analysed here, the runoff coefficient that gives a perfect match of the return periods is always larger than the median of the runoff coefficients that cause the maximum annual floods. For a system without runoff generation thresholds, one would have to choose a runoff coefficient that is exceeded in about 30% and 35% of the maximum annual flood events for wet and dry systems respectively (for T_Q=T_P=100 years). If a runoff generation threshold is present, the mapping depends on the threshold, the exceedance probabilities associated with $r_{1:1}$ have a wider range and the variability with the return period is higher. For T_Q=T_P=100 years one would have to choose a runoff coefficient that is exceeded in about 10% and 35% of the maximum annual flood events for low and high thresholds respectively. This means that the choice of a runoff coefficient for design, based on the distribution of the runoff coefficients of the maximum annual flood events, is more complex if the system has a threshold effect in runoff generation.

Comprehensive sensitivity analyses (not shown in this paper) indicate that the above results are generic and do not depend much on the particular rainfall model used. For a world where

- storm duration varies,
- rainfall intensities are distributed according to a positively skewed distribution,
- extreme rainfall intensity decreases with storm duration

and considering the simplifying assumptions made in this paper

- block rainfall,
- linear catchment response,
- random runoff coefficients and/or existence of threshold effects

the mapping of rainfall to flood return periods will always look very similar to the results shown here.

In ongoing work, we will deal with the effect of storm time-patterns and multiple storms on the mapping of rainfall to flood return periods.

Appendix A

Rainfall and rainfall-runoff models

We use a simplified version of the rainfall and rainfall-runoff models presented in Sivapalan et al. (2005). The main simplifications are that we do not consider seasonality and do not generate a continuous series of synthetic rainfall but a number of independent storms. As a stochastic rainfall model, we consider the Weibull distribution for storm durations t_r, whose probability density function is

$$f_{T_r}(t_r) = \frac{\beta_r}{\gamma_r}\left(\frac{t_r}{\gamma_r}\right)^{\beta_r-1}\exp\left(-\frac{t_r}{\gamma_r}\right)^{\beta_r}, \quad \text{(A1)}$$

with known parameters γ_r (scale) and β_r (shape). The first parameter is linked to δ_r, the mean storm duration, by the relationship

$$\gamma_r = \delta_r\left[\Gamma\left(1+\frac{1}{\beta_r}\right)\right]^{-1}. \quad \text{(A2)}$$

while the shape parameter is linked to the coefficient of variation of the distribution, that is

$$\mathrm{CV}_r = \sqrt{\frac{\Gamma(1+2/\beta_r)}{[\Gamma(1+1/\beta_r)]^2}-1}. \quad \text{(A3)}$$

We assume that the number of storm events per year is Poisson distributed with mean m. In particular, in this paper m=40, δ_r=6 h and β_r=0.7.

The rainfall intensity i within the storm is imposed to be constant (rectangular storms), while its distribution only depends on t_r, according to the gamma distribution

$$f_{I|T_r}(i|t_r) = \frac{\lambda}{\Gamma(\kappa)}(\lambda i)^{\kappa-1}\exp(-\lambda i), \quad \text{(A4)}$$

where parameters λ and κ are functions of t_r as

$$E[i|t_r] = a_1 t_r^{b_1} \quad \text{and} \quad \mathrm{CV}^2[i|t_r] = a_2 t_r^{b_2}, \quad \text{(A5)}$$

that means

$$\kappa = \frac{t_r^{-b_2}}{a_2} \quad \text{and} \quad \lambda = \frac{t_r^{-b_1-b_2}}{a_1 a_2}. \quad \text{(A6)}$$

In the following, we assume the parameters a_1, b_1, a_2 and b_2 to be known (Sivapalan et al., 2005 estimate them from data) and to be respectively equal to 1.05 mm h$^{-b_1-1}$, 0.01, 1.5 and −0.55.

The rainfall-runoff model is a standard linear reservoir with response time t_c with which the rainfall time series is convoluted. For a single storm, the transformation of rainfall to runoff can be expressed by the convolution integral of the exponential UH

$$q(t) = \frac{r_c}{t_c}\int_0^t i(t')\exp\left(-\frac{t-t'}{t_c}\right)dt', \quad \text{(A7)}$$

where $i(t)$ is the rainfall input time series, $q(t)$ is the resulting runoff time series and r_c is the runoff coefficient. Other components, such as base-flow and seasonality, are not considered. As rainfall intensity within the storm is assumed to be constant, the flood peak is

$$q_p = \Pi_Q(i, t_r, r_c) = r_c \cdot i \cdot \left[1-\exp\left(-\frac{t_r}{t_c}\right)\right], \quad \text{(A8)}$$

where we assume t_c as a constant. In this paper we consider always the same exponential UH with t_c=12 h.

Appendix B

Derived distribution approach

B1 Derived flood return period

Given the joint probability density function of rainfall intensity i, rainfall duration t_r and runoff coefficient r_c as $f_{I,T_r,R_c}(i, t_r, r_c)$, the probability for a given flood peak discharge Y to be less than or equal to q_p is

$$F_Y(q_p) = \Pr[Y \le q_p] = \\ = \int\int\int_R f_{I,T_r,R_c}(i, t_r, r_c)\,di\,dt_r\,dr_c, \quad \text{(B1)}$$

where R is the region of the (i, t_r, r_c) space for which the combination of these three values is transformed into a peak smaller than or equal to q_p by the rainfall-runoff model.

In the case of storm intensity being dependent on storm duration but runoff coefficient being independent, applying the Bayes theorem, the integral of Eq. (B1) simplifies to

$$F_Y(q_p) = \int_0^1\int_0^\infty F_{I|T_r}\left(\Pi_Q^{-1}(q_p, t_r, r_c)|t_r\right)\cdot \\ \cdot f_{T_r}(t_r) f_R(r_c)\,dt_r\,dr_c, \quad \text{(B2)}$$

where $F_{I|T_r}(.|t_r)$ is the conditional cumulative distribution of rainfall intensities conditioned on t_r, and $f_{T_r}(t_r)$ and $f_R(r_c)$ are the probability density functions of t_r and r_c. This is the case discussed in Sect. 4.1.

When there is a dependence between the event runoff coefficient and the storm event, for the relationship between joint and conditional probability density functions (e.g. Kottegoda and Rosso, 1997, p. 126), the joint distribution of I, T_r and R_c is given by:

$$f_{I,T_r,R_c}(i,t_r,r_c) = f_{R_c|I,T_r}(r_c|i,t_r)\cdot \cdot f_{I|T_r}(i|t_r)f_{T_r}(t_r)\,. \quad \text{(B3)}$$

and the integral of Eq. (B1) simplifies to

$$F_Y(q_p)=\int_0^\infty\int_0^\infty F_{R_c|I,T_r}\left(\Pi_Q^{-1}(q_p,t_r,r_c)|i,t_r\right)\cdot \cdot f_{I|T_r}(i|t_r)\cdot f_{T_r}(t_r)didt_r\,. \quad \text{(B4)}$$

This formulation of $F_Y(q_p)$ is particularly convenient when the non-linear threshold relationship between the event runoff coefficient and the storm event of Sect. 4.2 holds. In this case the space R of integration in Eq. (B1) is represented in Fig. B1. The region R is the one above the black surface, that provides a representation of the rainfall-runoff model expressed by Eq. (A8). This surface corresponds to one flood peak q_p and is a 3-D representation of the curve in Fig. 1 of Wood (1976) (here also r_c is taken into account). The surface corresponding to the threshold V^* is shown in grey. Below the grey surface ($V{=}i\,t_r{<}V^*$) the probability distribution of the runoff coefficient has parameters δ_{c_1} and σ_{c_1}; above, δ_{c_2} and σ_{c_2}. The integration of Eq. (B4) can then be easily divided into two parts considering these two separate regions.

Assuming the number of independent floods in a year to be Poisson distributed with mean m, the cumulative distribution function of the annual maximum flood Q is

$$F_Q(q_p) = \exp\left\{-m\left[1-F_Y(q_p)\right]\right\}\,. \quad \text{(B5)}$$

The same result can also be expressed in terms of the return period (in years):

$$T_Q = \left\{1-F_Q(q_p)\right\}^{-1}\,. \quad \text{(B6)}$$

B2 Derived storm return period

As explained in Viglione and Blöschl (2009), we derive the return period of storms referring to the IDF-based methodology. If we let a random variable I denote the rainfall intensity of storms averaged over the aggregation level t_{IDF}, the probability that this intensity is lower or equal to ϕ is called $F_I(\phi,t_{\mathrm{IDF}})$. The cumulative distribution of I (defined for a single t_{IDF}) is then

$$F_I(\phi,t_{\mathrm{IDF}}) = \Pr[I\le\phi] = \int\int_{R'} f_{I,T_r}(i,t_r)didt_r\,, \quad \text{(B7)}$$

where R' is the region of the (i,t_r) space such that the combination of these two values is transformed into a value smaller than or equal to ϕ by the IDF filter with aggregation level t_{IDF}. The result of the rectangular filtering can be written as:

$$\phi = \Pi_P(i,t_r) = \begin{cases} i & \text{if} \quad t_{\mathrm{IDF}} \le t_r \\ i\cdot t_r/t_{\mathrm{IDF}} & \text{if} \quad t_{\mathrm{IDF}} > t_r \end{cases}\,. \quad \text{(B8)}$$

so that Eq. (B7) can be simplified to

$$F_I(\phi,t_{\mathrm{IDF}}) = \int_0^\infty F_{I|T_r}\left(\Pi_P^{-1}(\phi,t_r)|t_r\right)f_{T_r}(t_r)dt_r\,, \quad \text{(B9)}$$

where $\Pi_P^{-1}(\phi,t_r)$ is the inverse of Eq. (B8) and expresses the intensity of a storm of duration t_r that has average intensity ϕ over the aggregation level t_{IDF}. If we denote by P the annual maximum rainfall intensity of storms averaged over the aggregation level t_{IDF}, then the probability distribution of P is

$$F_P(\phi,t_{\mathrm{IDF}}) = \exp\left\{-m\left[1-F_I(\phi,t_{\mathrm{IDF}})\right]\right\}\,, \quad \text{(B10)}$$

and

$$T_{\mathrm{IDF}}(\phi,t_{\mathrm{IDF}}) = \left\{1-F_P(\phi,t_{\mathrm{IDF}})\right\}^{-1} \quad \text{(B11)}$$

is the return period of storms with average intensity ϕ over the aggregation level t_{IDF}. This equation represents the IDF curves.

In our simplified world, the return period of individual storms can now be read off the IDF curve as $T_{\mathrm{IDF}}(\phi{=}i,\ t_{\mathrm{IDF}}{=}t_r)$. The return period T_P of the storms that

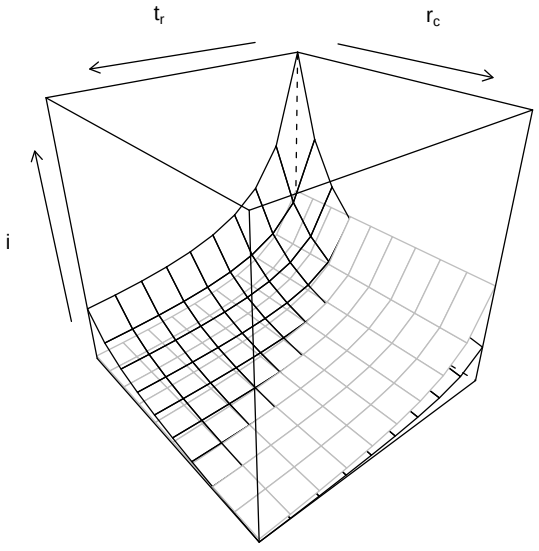

Fig. B1. Representation of the surfaces corresponding to the threshold rainfall-volume V^* (grey) and to one flood peak q_p (black) in the (t_r, i, r_c) space (storm duration, storm intensity, runoff coefficient).

produce the maximum annual peaks q_p (here called flood-producing storms) is then

$$T_P = T_{\mathrm{IDF}}(\phi = \Pi_Q^{-1}(q_p, t_r = t_{\mathrm{IDF}}, r_c),\ t_{\mathrm{IDF}} = t_r) \qquad \text{(B12)}$$

where $\Pi_Q^{-1}(.)$ is the storm intensity that, for given t_r, r_c and t_c, produces the flood peak q_p.

Acknowledgements. Financial support from the EC (Project no. 037024, HYDRATE), from the APART project of the Austrian Academy of Sciences and from the FWF project P18993-N10 are acknowledged. We would also like to thank Attilio Castellarin, Eric Gaume and Jon Olav Skøien for their useful comments on the manuscript in HESSD.

Edited by: A. Montanari

References

Alfieri, L., Laio, F., and Claps, P.: A simulation experiment for optimal design hyetograph selection, Hydrol. Process., 22, 813–820, 2008.

Bradley, A. A. and Potter, K. W.: Flood frequency analysis of simulated flows, Water Resour. Res., 28, 2375–2385, 1992.

Cerdan, O., Le Bissonnais, Y., Govers, G., Leconte, V., Van Oost, K., Couturier, A., King, C., and Dubreuil, N.: Scale effects on runoff from experimental plots to catchments in agricultural areas in Normandy, J. Hydrol., 299, 4–14, 2004.

Chow, V. T., Maidment, D. R., and Mays, L. W.: Applied Hydrology, Civil Engineering Series, McGraw-Hill Book Company, int. edn., 572 pp., 1988.

Dos Reis Castro, N. M., Auzet, A. V., Chevallier, P., and Leprun, J. C.: Land use change effects on runoff and erosion from plot to catchment scale on the basaltic plateau of Southern Brazil, Hydrol. Process., 13, 1621–1628, 1999.

DVWK: Hochwasserabflüsse, Kommissionsvertrieb Wirtschafts- und Verlagsgesellschaft Gas und Wasser, Bonn, 1999.

Gottschalk, L. and Weingartner, R.: Distribution of peak flow derived from a distribution of rainfall volume and runoff coefficient, and a unit hydrograph, J. Hydrol., 208, 148–162, 1998.

Gutknecht, D., Reszler, C., and Blöschl, G.: Das Katastrophenhochwasser vom 7. August 2002 am Kamp – eine erste Einschätzung (The August 7, 2002 – flood of the Kamp – a first assessment), Elektrotechnik und Informationstechnik, 119, 411–413, 2002.

Houghton-Carr, H.: Restatement and application of the Flood Studies Report rainfall-runoff method, in: Flood Estimation HandBook, Institute of Hydrology Crowmarsh Gifford, Wallingford, Oxfordshire, 4, 288 pp., 1999.

Kottegoda, N. T. and Rosso, R.: Statistics, Probability, and Reliability for Civil and Environmental Engineers, McGraw-Hill Companies, international edn., 735 pp., 1997.

Koutsoyiannis, D., Kozonis, D., and Manetas, A.: A mathematical framework for studying rainfall intensity-duration-frequency relationships, J. Hydrol., 206, 118–135, 1998.

Kusumastuti, D. I., Struthers, I., Sivapalan, M., and Reynolds, D. A.: Threshold effects in catchment storm response and the occurrence and magnitude of flood events: implications for flood frequency, Hydrol. Earth Syst. Sci., 11, 1515–1528, 2007, http://www.hydrol-earth-syst-sci.net/11/1515/2007/.

Merz, R. and Blöschl, G.: A regional analysis of event runoff coefficients with respect to climate and catchment characteristics in Austria, Water Resour. Res., 45, W01405, doi:10.1029/2008WR007163, 2009.

Merz, R., Blöschl, G., and Parajka, J.: Spatio-temporal variability of event runoff coefficients, J. Hydrol., 331, 591–604, 2006.

Naef, F.: Der Abflusskoeffzient: einfach und praktisch?, in: Aktuelle Aspekte in der Hydrologie, vol. 53 of Zurcher Geographische Schriften, Verlag Geographisches Institut ETH Zurich, 193–199, 1993.

Packman, J. C. and Kidd, C. H. R.: A logical approach to the design storm concept, Water Resour. Res., 16, 994–1000, 1980.

Pilgrim, D. H. (ed.): Australian Rainfall and Runoff, A Guide to Flood Estimation, The Institution of Engineers, ACT, Australia, 1987.

Pilgrim, D. H. and Cordery, I.: Rainfall temporal patterns for design floods, J. Hyd. Div.-ASCE, 101, 81–95, 1975.

Pilgrim, D. H. and Cordery, I.: Flood Runoff, in: HandBook of Hydrology, edited by: Maidment, D. R., McGraw-Hill Companies, international edn., chap. 9, 42 pp., 1993.

Reed, D. W.: Procedures for flood frequency estimation, in: Flood Estimation HandBook, Institute of Hydrology Crowmarsh Gifford, Wallingford, Oxfordshire, 1, 108 pp., 1999.

Sherman, L.: Streamflow from rainfall by unit hydrograph method, Eng. News-Rec., 108, 501–505, 1932.

Sieker, F. and Verworn, H. R.: Wird der Blockregen als Bemessungsregen dem Postulat "Regenhäufigkeit=Abflußhäufigkeit" gerecht?, Wasser und Boden, 2, 52–55, 1980.

Sivapalan, M., Blöschl, G., Merz, R., and Gutknecht, D.: Linking flood frequency to long-term water balance: Incorporating effects of seasonality, Water Resour. Res., 41, W06012, doi:10.1029/2004WR003439, 2005.

Struthers, I. and Sivapalan, M.: A conceptual investigation of process controls upon flood frequency: role of thresholds, Hydrol. Earth Syst. Sci., 11, 1405–1416, 2007, http://www.hydrol-earth-syst-sci.net/11/1405/2007/.

Viglione, A. and Blöschl, G.: On the role of storm duration in the mapping of rainfall to flood return periods, Hydrol. Earth Syst. Sci., 13, 205–216, 2009, http://www.hydrol-earth-syst-sci.net/13/205/2009/.

Western, A., Blöschl, G., and Grayson, R.: How well do indicator variograms capture the spatial connectivity of soil moisture?, Hydrol. Process., 12, 1851–1868, 1998.

Wood, E. F.: An analysis of the effects of parameter uncertainty in deterministic hydrologic models, Water Resour. Res., 12, 925–932, 1976.

Zehe, E. and Blöschl, G.: Predictability of hydrologic response at the plot and catchment scales: Role of initial conditions, Water Resour. Res., 40, W10202, doi:10.1029/2003WR002869, 2004.

Zehe, E., Elsenbeer, H., Lindenmaier, F., Schulz, K., and Blöschl, G.: Patterns of predictability in hydrological threshold systems, Water Resour. Res., 43, W07434, doi:10.1029/2006WR005589, 2007.